[redacted] CONFIDENTIAL

NACA RM E55K16

TECH LIBRARY KAFB, NM
0144067

6546

NACA

RESEARCH MEMORANDUM

Reg # 4953

WEIGHT-FLOW AND THRUST LIMITATIONS DUE TO USE OF ROTATING COMBUSTORS IN A TURBOJET ENGINE

By Erwin A. Lezberg, Perry L. Blackshear, Jr., and Warren D. Rayle

Lewis Flight Propulsion Laboratory
Cleveland, Ohio

Classification cancelled (or changed to UNCLASSIFIED)
By Authority of NASA Tech Pub Announcement #39
(OFFICER AUTHORIZED TO CHANGE)
By ..... 16 Feb 61
GRADE OF OFFICER MAKING CHANGE)
16 Mar 61
DATE

CLASSIFIED DOCUMENT

This material contains information affecting the National Defense of the United States within the meaning of the espionage laws, Title 18, U.S.C., Secs. 793 and 794, the transmission or revelation of which in any manner to an unauthorized person is prohibited by law.

NATIONAL ADVISORY COMMITTEE FOR AERONAUTICS

WASHINGTON

August 17, 1956

[redacted] CONFIDENTIAL [redacted]

TECH LIBRARY KAFB, NM
0144067

NATIONAL ADVISORY COMMITTEE FOR AERONAUTICS

RESEARCH MEMORANDUM

WEIGHT-FLOW AND THRUST LIMITATIONS DUE TO USE OF ROTATING COMBUSTORS IN A TURBOJET ENGINE

3668

By Erwin A. Lezberg, Perry L. Blackshear, Jr., and Warren D. Rayle

SUMMARY

Recent research on high-energy fuels indicates that those containing boron are among the most promising. Two consequences of this fact that may influence future engine design are: (1) Exhaust products may be expected to adhere to stationary parts but not to rotating parts. (2) Reactivity of fuel is high, permitting small combustors. This paper suggests an engine configuration that is intended to minimize the difficulty caused by (1) and exploit (2). In the engine suggested, one stage of the compressor, the combustor, and the turbine are combined in a single rotating unit resembling a nest of rotating ram jets.

Component efficiencies of such an engine are assigned, and its performance is compared with that of a single-stage turbine engine. The rotating-combustor unit passes lower weight flows and gives less thrust per unit frontal area than the conventional turbojet engine. At all Mach numbers of 1.5 and less, the thrust of the rotating-combustor engine is inferior to that of the turbojet by 28 percent or more. At Mach numbers of 2.3 and presumably above, this thrust difference becomes less than 12 percent. The specific fuel consumption is somewhat higher than that for the conventional turbojet engine over the lower range of compression ratios.

INTRODUCTION

The use of fuels having higher heating values than hydrocarbons to increase the performance of jet-powered aircraft has been examined (refs. 1 and 2) and appears promising. In these investigations, the high-energy fuels have been applied to engine types originally designed for use with hydrocarbon fuels. Some of these fuels contain boron (ref. 3) and, hence, form liquid or solid products on combustion with air. Boron oxide

may be expected to deposit extensively on stationary surfaces in turbojet engines, such as combustor linings, stator blades, and exhaust nozzles. There is reason to believe that high centrifugal forces, such as are found on rotor blades, will help maintain clean surfaces (unpublished NACA data).

The high reactivity of the high-energy fuels, some of which have flame speeds in the order of 100 times that of hydrocarbons (ref. 4), suggests that reductions in combustor volume might be achieved. An engine having rotating combustor passages, which could take advantage of weight savings due to shorter combustors, has been suggested and is shown schematically in figure 1. The engine may be considered as a turbojet engine in which the last compressor stage, the combustors, and the turbine are replaced by a single rotating unit consisting of a diffuser cascade, combustor passages, and reaction nozzles. Stators downstream of the rotor remove exit whirl when necessary. 3668

The engine, without precompression, might be viewed as a nest of rotating ram jets with only enough exit whirl to balance friction losses. If blade relative Mach numbers on the order of 1.5 to 3 could be achieved, compression ratios and, hence, cycle efficiencies equal to those of the conventional turbojet engine could be obtained in theory. Since current turbine blade or rotor stress limitations preclude such speeds, staged compression and, therefore, whirl in the rotor exhaust gases are necessary for acceptable compression ratios.

In the analysis that follows, component efficiencies are assigned the engine of figure 1; and weight flow, thrust, and specific fuel consumption are calculated. These results are compared to those of a single-stage air-cooled turbine engine having comparable component efficiencies.

The assumption is made for the rotojet that the combustor passage walls are kept cool by stratification of air and combustion products. Cooling losses are not charged to the rotojet, but are charged to the turbojet where such stratification is impossible.

The comparison between the rotojet and turbojet engines is made over a flight Mach number range of zero to 2.3 and at turbine-inlet temperatures of 2500° and 3500° R.

The idea of utilizing centrifugal forces to keep combustor surfaces free of oxide deposits has been informally discussed in the high-energy fuels field for years. The reaction turbine dates back to the Greek aeolipile which antedates Hero's turbine of 130 B.C. In modern times, Nernst, Lorin, and a host of others have proposed engines involving reaction turbines, in some of which combustors revolved. In the present work, the ancient design is carried to an extreme in flow per unit frontal area.

3668

CW-1 back

SYMBOLS

A	area, sq ft
A_F	turbine tip frontal area, sq ft
a'	stagnation sound speed, $\sqrt{kgRT'}$, ft/sec
a'_{cr}	$\sqrt{\frac{2k}{k+1} gRT'}$, ft/sec
C_D	flameholder drag coefficient, $(p''_2 - p''_3)/q$
C_V	exhaust-nozzle velocity coefficient
c_p	specific heat at constant pressure, Btu/(lb)(°R)
E	work, ft-lb/lb
F	engine thrust, lb
g	acceleration due to gravity, 32.2 ft/sec^2
$\overline{H}$	lower heating value of fuel, Btu/lb
J	mechanical equivalent of heat, 778.2 ft-lb/Btu
k	ratio of specific heats
M	Mach number relative to rotor blades
M_0	flight Mach number
p	absolute pressure, lb/sq ft
q	dynamic head, $\rho_g V^2/2g$, lb/sq ft
R	gas constant, 53.3 ft-lb/(lb)(°R)
$\frac{r_h}{r_t}$	hub-tip radius ratio
sfc	specific fuel consumption, lb/(hr)(lb)
T	absolute temperature, °R

U blade velocity, ft/sec

V absolute gas velocity, ft/sec

W relative gas velocity, ft/sec

w weight-flow rate, lb/sec

β reaction-nozzle-jet angle, deg

δ ratio of stagnation pressure to NACA standard sea-level pressure of 2116 lb/sq ft

η efficiency

θ ratio of stagnation temperature to NACA standard sea-level temperature of 518.7° R

ρ density, lb/cu ft

σ blade centrifugal stress, psi

ψ blade stress taper factor

Subscripts:

a air

an annular

B combustor

b blade material

C compressor

ca cooling air

g gas

i ideal

j jet

m mean radius

n reaction nozzle

T turbine

3668

u tangential component

x axial component

0 free stream

1 compressor inlet

2 compressor discharge

3 plane of flameholder

3a combustor exit

4 downstream of reaction nozzle at stator inlet; turbine rotor inlet

5 rotojet stator exit; turbine rotor exit

6 exhaust-nozzle inlet

Superscripts:

' stagnation state relative to stationary coordinates

" stagnation state relative to rotating coordinates

ANALYSIS

The rotating-combustor engine (rotojet) used for this analysis is shown schematically in figure 1. A single-stage turbine engine employing turbine cooling is used for comparison (fig. 2).

Stress Limitations

For both turbojet and rotojet engines, the stress at the rotor blade roots was limited to 44,000 psi. This value is the stress-rupture limit for S-816 alloy for 100-hour life and a blade root temperature of about 1300° F taken without safety factor (ref. 5). For the rotojet, this blade temperature was assumed to be achievable with temperature stratification. For the turbojet, convection-cooled stators and rotors were assumed with cooling-air requirements of 5 percent of the total air flow for a turbine-inlet total temperature of 2500° R and 15 percent of the total air flow for a temperature of 3500° R. The 2500° R temperature represents an operating temperature achievable at present with turbine cooling. The 3500° R temperature was taken as an extreme case to illustrate the maximum gains possible if temperature stratification is used successfully for cooling the rotor blades.

The mean blade speed was calculated from the following equation (taken from ref. 6) for a hub-tip radius ratio of 0.5, a blade density of 490 pounds per cubic foot, and a blade taper factor of 0.69:

$$U_m = \frac{1 + \frac{r_h}{r_t}}{2} \sqrt{\frac{288g\sigma}{\psi\rho_b \left[1 - \left(\frac{r_h}{r_t}\right)^2\right]}} \tag{1}$$

3668

Assumptions and Range of Analysis

The following assumptions were made for both engines:

(1) Constantly variable inlet and nozzle geometry for on-design operation

(2) Specific heat at constant pressure $c_p = 0.24$ Btu/(lb)(°R)

(3) Compressor adiabatic efficiency $\eta_C = \eta_C' = 0.85$

(4) Turbine adiabatic efficiency $\eta_T = \eta_n = 0.85$

(5) Combustion efficiency $\eta_B = 0.95$

(6) Lower heating value of fuel $\overline{H} = 18{,}900$ Btu/lb

(7) Exhaust-nozzle velocity coefficient $C_V = 0.95$

(8) Inlet total-pressure recoveries of 0.95 for subsonic operation, and theoretical values for double-angle-cone inlet for supersonic operation

Following is the range of the analysis:

(1) Flight Mach number $M_0 = 0$ at sea level

(2) Flight Mach number $M_0 = 0.9$, 1.5, and 2.3 at tropopause

(3) Turbine-inlet total temperatures of 2500° and 3500° R

(4) Turbine hub-tip radius ratio $r_h/r_t = 0.5$, and tip speed of 1263 ft/sec

(5) Angle of reaction-nozzle jet with direction of rotation $\beta = 20^{\circ}$ to 45°

(6) Axial Mach numbers downstream of rotor $M_{4,x} = 0.6, 0.7, 0.8,$ and 1.0 for rotojet, 0.7 for turbojet

Rotojet Analysis Methods

3668

Weight flow and work. - The weight-flow limitations of the rotojet were calculated from the following equation and assumed values of axial Mach number downstream of the turbine rotor and angle of reaction-nozzle jet:

$$\frac{w_a a_4''}{p_4''} = \frac{kgA_{an}M_{4,x}}{\left(1 + \frac{k-1}{2}\frac{M_{4,x}^2}{\sin^2\beta}\right)^{\frac{k+1}{2(k-1)}}} \tag{2}$$

(The derivation of equation (2) is given in appendix A.) The corrected weight flow in terms of the stagnation conditions at the compressor inlet and the turbine rotor frontal area is then given by

$$\frac{w_a\sqrt{\theta_1}}{A_F\delta_1} = \frac{w_a a_4''}{A_{an}p_4''}\frac{p_4''}{p_1'}\sqrt{\frac{T_1'}{T_4''}}\left[1 - \left(\frac{r_h}{r_t}\right)^2\right]\frac{2116}{\sqrt{518.7\ kgR}} \tag{3}$$

where p_4''/p_1' is the engine total-pressure ratio, and T_1'/T_4'' is the engine total-temperature ratio.

The work of the reaction turbine is given by

$$E_T' = \frac{U_m}{g}\left(\frac{M_{4,x}a_{3a}''\cot\beta}{\sqrt{1 + \frac{k-1}{2}\frac{M_{4,x}^2}{\sin^2\beta}}} - \frac{U_m}{2}\right) \tag{4}$$

By equating the turbine work to the compressor work, the compressor total-pressure ratio relative to the rotor is determined:

$$\frac{p_2''}{p_1'} = \left(\frac{E_T'\eta_C'}{Jc_p\ T_1'} + 1\right)^{\frac{k}{k-1}} \tag{5}$$

where η_C' is defined by

$$\eta_C' = \frac{\left(\frac{p_2''}{p_1'}\right)^{\frac{k-1}{k}} - 1}{\frac{T_2''}{T_1'} - 1}$$

(Equations (4) and (5) are derived in appendix A.)

3668

Engine losses. - Combustor total-pressure losses relative to the rotor were determined by dividing the losses into a momentum pressure loss from stations 3 to 3a and a flameholder drag loss from stations 2 to 3. The Mach number at the combustor exit M_{3a} was determined from the Mach number of the jet M_4 and the isentropic area change functions. The combustor total-temperature ratio was determined from the assumed value of reaction-nozzle-inlet total temperature and the total temperature at the compressor outlet relative to the rotor, which is found from

$$T_2'' = T_1' + \Delta T_C' - \frac{U_m^2}{2gJc_p} = T_1' + \Delta T_C'' \tag{6}$$

Momentum pressure losses and the Mach number at the plane of the flameholder were calculated with the Rayleigh line relations. Flameholder drag losses were calculated by assuming $C_D = 4q$ and writing an approximate equation for the total-pressure ratio across the flameholder in terms of the Mach number at station 3:

$$\frac{p_2''}{p_3''} \cong \frac{5.6\ M_3^2}{\sqrt{1 + 11.2\ M_3^2} - 1} \tag{7}$$

The total-pressure losses in and downstream of the rotating reaction nozzles and in the stator stage following were lumped together into a total-pressure efficiency. The stator stage was assumed to completely recover the whirl energy.

The total-pressure ratio across the reaction nozzle was assumed to be a function only of the static-pressure ratio across the nozzles and the nozzle efficiency:

$$\frac{p''_{3a}}{p''_4} = \left[\left(\frac{p_{3a}}{p_4}\right)^{\frac{k-1}{k}} (1 - \eta_n) + \eta_n\right]^{\frac{k}{k-1}} \tag{8}$$

(Equations (7) and (8) are derived in appendix B.)

Performance parameters. - For complete expansion from the total pressure at station 6 to ambient static pressure, the jet velocity is given by

$$V_j = C_V \sqrt{T'_6 2gJc_p\left[1 - \left(\frac{p_0}{p'_6}\right)^{\frac{k-1}{k}}\right]} \tag{9}$$

Corrected thrust $F/A_F\delta$ is then equal to the product of corrected weight flow $w_a\sqrt{\theta}/A_F\delta$ and corrected impulse $(V_j - V_0)/g\sqrt{\theta}$, when δ and θ have their usual significance and V_0 is the flight speed.

Specific fuel consumption is determined from

$$sfc = \frac{c_p\,(T''_{3a} - T''_2)}{\frac{V_j - V_0}{g}\,\eta_B\,\overline{H}\,3600} \tag{10}$$

Turbojet Analysis Methods

For the turbojet engine used for comparison with the rotojet, a turbine operating at limiting loading is assumed, with the turbine determining the mass flow through the engine. An exit critical velocity ratio of 0.7 is assumed for the turbine as the value for limiting loading (ref. 7). The tangential component of velocity downstream of the turbine rotor is assumed equal to zero for all values of the change of tangential velocity across the rotor equal to or greater than twice the blade speed. The change in tangential velocity was allowed to increase beyond this value, but the exit-whirl kinetic energy was not considered recoverable.

Weight flow and work. - The turbine weight flow was calculated with the relations developed in reference 8:

$$w_a = \rho_g a''_{cr} A_{an} \frac{\rho_g V_x}{\rho'_g\, a'_{cr}} \tag{11}$$

where

$$\frac{\rho_g V_x}{\rho_g' a_{cr}'} = \frac{V_x}{a_{cr}'}\left\{1 - \frac{k-1}{k+1}\left[\left(\frac{V_x}{a_{cr}'}\right)^2 + \left(\frac{V_u}{a_{cr}'}\right)^2\right]\right\}^{\frac{1}{k-1}} \tag{12}$$

and the critical velocity a_{cr}' is defined as

$$a_{cr}' \equiv \sqrt{\frac{2k}{k+1} gRT'} \tag{13}$$

The value of V_x/a_{cr}' was assumed constant at 0.7, and values of V_u/a_{cr}' were calculated for assumed values of the compressor total-pressure ratio from the turbine velocity diagram and the Euler work equation.

The turbine work in terms of compressor total-pressure ratio is

$$E_T = c_p(T_{3a}' - T_5') = \left(1 + \frac{w_{ca}}{w_a}\right)\frac{T_1' c_p}{\eta_C}\left[\left(\frac{p_2'}{p_1'}\right)^{\frac{k-1}{k}} - 1\right] \tag{14}$$

where w_{ca}/w_a is the turbine cooling-air ratio.

The required change in the tangential component of velocity across the turbine rotor is given by the Euler equation:

$$E_T = \frac{U_m}{g}(V_{u,4} - V_{u,5}) \tag{15}$$

When $V_{u,5}$ has values other than zero,

$$V_{u,5} = E_T \frac{g}{U_m} - 2U_m \tag{16}$$

Then V_u/a_{cr}' can be determined from equations (13), (14), and (16) and the turbine-inlet total temperature T_{3a}'.

Equation (11) can be rewritten in terms of the total pressure and temperature at the turbine rotor exit and the turbine frontal area:

$$\frac{w_a\sqrt{T_5'}}{A_F p_5'} = \frac{\rho_g V_x}{\rho_g' a_{cr}'}\sqrt{\frac{2k}{k+1}\frac{g}{R}}\left[1 - \left(\frac{r_h}{r_t}\right)^2\right] \tag{17}$$

At the compressor inlet, the weight flow can be rewritten in terms of the total-temperature and -pressure ratios through the engine:

$$\frac{w_a\sqrt{T_1'}}{A_F p_1'} = \frac{\rho_g V_x}{\rho_g' a_{cr}'}\sqrt{\frac{2k}{k+1}\frac{g}{R}}\left[1 - \left(\frac{r_h}{r_t}\right)^2\right]\sqrt{\frac{T_{3a}'}{T_5'}\frac{T_1'}{T_{3a}'}}\frac{p_5'}{p_{3a}'}\frac{p_{3a}'}{p_2'}\frac{p_2'}{p_1'}\left(1 + \frac{w_{ca}}{w_a}\right) \tag{18}$$

Substituting $\sqrt{\theta_1} = \sqrt{T_1'/518.7}$ and $\delta_1 = p_1'/2116$ gives the equivalent weight flow:

$$\frac{w_a\sqrt{\theta_1}}{A_F\delta_1} = \frac{\rho_g V_x}{\rho_g' a_{cr}'}\sqrt{\frac{2k}{k+1}\frac{g}{R}}\left[1 - \left(\frac{r_h}{r_t}\right)^2\right]\sqrt{\frac{T_{3a}'}{T_5'}\frac{T_1'}{T_{3a}'}}\frac{p_5'}{p_{3a}'}\frac{p_{3a}'}{p_2'}\frac{p_2'}{p_1'}\frac{2116}{\sqrt{518.7}}\left(1 + \frac{w_{ca}}{w_a}\right) \tag{19}$$

Engine losses. - Combustor total-pressure losses were determined by a trial-and-error solution using a plot of combustor reference velocity against total-pressure ratio across the combustor (ref. 9). A reference velocity was assumed and the combustor total-pressure ratio substituted in equation (19) to determine an equivalent weight flow. A new reference velocity was then calculated and the process continued until no further change in $w_a\sqrt{\theta_1}/A_F\delta_1$ resulted.

The turbine total-pressure ratio was calculated from the equation for turbine adiabatic efficiency:

$$\eta_T = \frac{1 - \frac{T_5'}{T_{3a}'}}{1 - \left(\frac{p_5'}{p_{3a}'}\right)^{\frac{k-1}{k}}} \tag{20}$$

Losses due to cooling air for the turbine were treated by assuming the cooling air as bypassed around the turbine. A larger turbine work term was therefore required for each pound of compressor air flow. The cooling air was assumed to be dumped downstream of the turbine at the total pressure of the main gas stream and at the compressor-outlet total temperature.

The increase in mass flow due to fuel addition was neglected.

The engine total-pressure ratio and exhaust-nozzle-inlet total temperature were corrected for whirl losses at the turbine outlet by crediting these quantities with the axial-velocity component only.

The engine-inlet total-pressure ratio and exhaust-nozzle velocity coefficient were the same for both engines. The performance parameters were calculated in the same manner as for the rotojet engine.

RESULTS

Effect of Reaction-Nozzle-Jet Angle on Rotojet Compression Ratio

The effect of reaction-nozzle-jet angle on rotojet compression ratio is shown in figure 3 for a turbine-inlet total temperature of 2500° R for a variety of turbine-exit axial Mach numbers and flight Mach numbers. Exit axial Mach number has a small effect on attainable compression ratio. The pressure ratio attainable goes up sharply as reaction-nozzle-jet angle approaches the tangential. (This increase in pressure ratio is at the expense of through-flow, as will be shown subsequently.)

Effect of Turbine-Exit Axial Mach Number on Rotojet Performance

Calculations were performed in the rotojet analysis for axial Mach numbers downstream of the reaction turbine ranging from 0.6 to 1.0. The effect of varying the axial Mach number on the specific fuel consumption, corrected thrust, and corrected weight flow as functions of compressor total-pressure ratio for the rotojet at a flight Mach number of 1.5 and a turbine-inlet total temperature of 2500° R is shown in figure 4. The specific fuel consumption is very little affected by the variations in axial Mach number downstream of the turbine. Although corrected thrust and weight flow maximize at an axial Mach number of 0.8, the change over the conventional limiting axial Mach number of 0.7 employed in turbojet analyses is so small that, for the sake of consistency, the data that follow are restricted to turbine-exit axial Mach numbers of 0.7.

Comparison of Rotojet and Turbojet Performance

Turbine-inlet temperature of 2500° R. - Specific fuel consumption, corrected thrust, and corrected weight flow are plotted against compressor total-pressure ratio for the rotojet and the turbojet at four different flight conditions in figure 5. The compression ratios are related to reaction-nozzle-jet angle by figure 3. Compressor-outlet total pressure and turbine-inlet total temperature are taken with respect to the rotating combustor walls for the rotojet and with respect to stationary coordinates for the turbojet. This means that the static pressure at

which heat is added is approximately the same in both engines; hence, the two engines have almost the same thermodynamic cycle.

For all flight conditions and compression ratios covered, the thrust and weight flow are higher for the turbojet than for the rotojet engine. Specific fuel consumption for the turbojet is slightly lower for the lower range of compression ratios. The turbojet shows higher specific fuel consumption at higher compression ratios. To the right of the vertical dash-dot lines in the figures, the tangential component of the turbine nozzle velocity in the turbojet exceeds twice the mean blade speed, and the residual velocity appears as whirl and is considered to be unavailable for producing thrust. The factors contributing to these differences are (1) differences in combustor total-pressure losses between the two engines, (2) the effects of bypassing cooling air in the turbojet, and (3) whirl losses for the turbojet at higher compression ratios due to the unfavorable ratio of jet velocity to blade speed.

The thrust of the rotojet engine approaches that of the turbojet at the lower compression ratios and highest flight speed.

Turbine-inlet temperature of 3500° R. - Rotojet and turbojet performance is compared over the same range of flight Mach numbers and altitudes at a turbine-inlet temperature of 3500° R in figure 6. The results are substantially the same as for the 2500° R turbine-inlet temperature. The blade temperatures for the rotojet are assumed to remain at a maximum of 1300° F by temperature stratification alone. The comparison serves only to show the gains that would result if temperature stratification could be achieved.

Performance of Fixed-Geometry Rotojet Engine

At high flight Mach numbers, the thrust and weight flow of the rotojet maximize at fairly low compression ratios. This fact indicates that an engine having an acceptable compression ratio might be designed with a single transonic compressor stage preceding the rotor diffuser cascade.

The fixed-geometry performance for rotojet engines designed for flight Mach numbers of 0 to 2.3 and turbine-inlet temperatures of 2500° and 3500° R was determined, and the results are presented in figure 7. Here the angle of the reaction-nozzle jet with the direction of rotation was held constant at the value for maximum thrust at the design Mach number, and the values of weight flow and compression ratio were determined at this blade angle for the other flight conditions. The values of weight flow for off-design performance are nowhere far from their peak values. The curves presented in figure 7 correspond to constant-rotational-speed operating lines on a compressor map and indicate that matching will not be a problem.

DISCUSSION

The rotojet performance calculations are contingent on component efficiencies that would have to result from a fairly substantial development program and the satisfactory application of temperature stratification for keeping the blades cool. If the components can be made to perform as assumed, there seems to be a range of application for an engine similar to the configuration discussed here, for high flight Mach numbers and moderately high turbine-inlet temperatures.

The practicability of such a unit depends on whether a rotating-combustor unit could be constructed to withstand the high stress value assumed without prohibitive weights. Another problem that would be encountered in the development of combustor passages operating at high centrifugal loadings would be the introduction and distribution of a liquid fuel. The fuel would have to be introduced so that it would not wet the walls to prevent fuel decomposition and burning off the metal surfaces. It appears that mixing would be promoted by the high centrifugal fields present, but secondary flows might cause appreciable losses. These are questions that can best be answered experimentally. Even if these problems could be solved satisfactorily, the attractiveness of such a unit diminishes considerably if the high-energy fuels can be used successfully in conventional turbojet engines for prolonged periods.

CONCLUSIONS

An engine that replaces a compressor stage, combustors, and turbine of a conventional turbine engine with a single rotating unit was compared with a turbojet engine over a range of operating conditions and design parameters. The turbojet shows higher air flow and higher thrust over the range of conditions covered. Specific fuel consumption of the rotojet is somewhat higher than that of the turbojet at the lower compression ratios. At all Mach numbers of 1.5 and lower, the thrust of the rotojet is inferior to that of the turbojet by 28 percent or more. At Mach numbers of 2.3 and presumably above, this thrust difference becomes less than 12 percent.

Lewis Flight Propulsion Laboratory
National Advisory Committee for Aeronautics
Cleveland, Ohio, November 21, 1955

APPENDIX A

CALCULATION OF ROTOJET WEIGHT-FLOW AND WORK PARAMETERS

The velocity diagram for the rotojet is shown in the following sketch, where V_2 is the absolute velocity from the last compressor stator stage, and V_4 is the absolute velocity leaving the reaction nozzles:

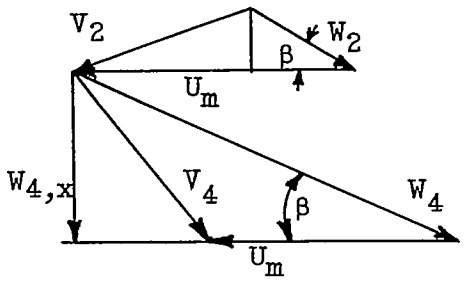

The weight flow of air at any station is given by

$$w_a = \rho_g A V \tag{A1}$$

At station 4, downstream of the reaction nozzles, the weight flow is determined by specifying the axial component of the jet velocity and the angle of the jet with the direction of rotation. The jet velocity becomes

$$W_4 = \frac{W_{4,x}}{\sin \beta} \tag{A2}$$

If A_{an} represents the turbine annulus area, $A_{an} \sin \beta$ is the jet area taken at 90° to the stream direction. From equation (A1),

$$w_a = \rho_{g,4} A_{an} \sin \beta \frac{W_{4,x}}{\sin \beta} \tag{A3}$$

In terms of Mach number and stagnation values for density and temperature,

$$w_a = \frac{\rho''_{g,4} A_{an} M_{4,x} \sqrt{kgRT''_4}}{\left(1 + \frac{k-1}{2} \frac{M^2_{4,x}}{\sin^2\beta}\right)^{\frac{k+1}{2(k-1)}}} \tag{A4}$$

Substituting $\rho''_g = p''/RT''$ and solving for the weight-flow parameter give

$$\frac{w_a a''_4}{p''_4} = \frac{kgA_{an} M_{4,x}}{\left(1 + \frac{k-1}{2} \frac{M^2_{4,x}}{\sin^2\beta}\right)^{\frac{k+1}{2(k-1)}}} \tag{2}$$

Since flow through the nozzles is assumed adiabatic, the weight flow of air for 1 square foot of turbine annulus area becomes

$$\frac{w_a a''_{3a}}{A_{an} p''_4} = \frac{kgM_{4,x}}{\left(1 + \frac{k-1}{2} \frac{M^2_{4,x}}{\sin^2\beta}\right)^{\frac{k+1}{2(k-1)}}} \tag{A5}$$

From the work equation, the net change in tangential momentum equals the turbine work:

$$E_T = \frac{U_m}{g} (W_4 \cos\beta - W_2 \cos\beta) \tag{A6}$$

where W_2 is the velocity relative to the rotor at the compressor exit, and W_4 is the velocity relative to the rotor at the turbine exit. For simplicity, the angle β is held the same for both inlet and outlet. Equating the work of compression to the turbine work,

$$E_C = Jc_p (T'_2 - T'_1) = \frac{U_m}{g} (W_4 \cos\beta - W_2 \cos\beta) \tag{A7}$$

The stagnation temperature at station 2 with respect to stationary coordinates is given by

$$T_2' = T_2 + \frac{V_2^2}{2gJc_p} \tag{A8}$$

where

3668

$$V_2^2 = W_2^2 \sin^2\beta + (U_m - W_2 \cos \beta)^2 = W_2^2 \sin^2\beta + U_m^2 - 2U_m W_2 \cos \beta + W_2^2 \cos^2\beta \tag{A9}$$

The stagnation temperature at station 2 relative to rotating coordinates is given by

$$T_2'' = T_2 + \frac{W_2^2}{2gJc_p} \tag{A10}$$

Subtracting equation (A10) from (A8) and substituting the value of V_2^2 in (A9) give

$$T_2' - T_2'' = \frac{U_m^2 - 2U_m W_2 \cos \beta}{2gJc_p} \tag{A11}$$

Since $(T_2' - T_1') = (T_2'' - T_1') + (T_2' - T_2'')$, the expression for the compressor work from equation (A7) becomes

$$E_C = Jc_p(T_2'' - T_1') + \frac{U_m^2 - 2U_m W_2 \cos \beta}{2g} = \frac{U_m}{g} (W_4 \cos \beta - W_2 \cos \beta) \tag{A12}$$

The work of compression from station 1 relative to the casing to station 2 (relative to the rotating combustors) is found by simplifying equation (A12) as follows:

$$E_C' = Jc_p(T_2'' - T_1') = \frac{U_m}{g} \left(W_4 \cos \beta - \frac{U_m}{2}\right) \tag{A13}$$

Writing W_4 in terms of the axial Mach number at station 4 and stagnation sound speed yields

$$W_4 = \frac{M_{4,x}}{\sin\beta} \frac{a_4''}{\sqrt{1 + \frac{k-1}{2}\frac{M_{4,x}^2}{\sin^2\beta}}} \tag{A14}$$

By substituting W_4 in equation (A13) and assuming adiabatic flow in the nozzles, the turbine work parameter is determined:

$$E_T' = \frac{U_m}{g}\left(\frac{M_{4,x}a_{3a}''\cot\beta}{\sqrt{1 + \frac{k-1}{2}\frac{M_{4,x}^2}{\sin^2\beta}}} - \frac{U_m}{2}\right) \tag{4}$$

3668

The compressor total-pressure ratio is related to the compressor work by

$$E_C' = \frac{Jc_pT_1'}{\eta_C'}\left[\left(\frac{p_2''}{p_1'}\right)^{\frac{k-1}{k}} - 1\right] = E_T' \tag{A15}$$

3668

CW-3 back

APPENDIX B

CALCULATION OF ROTOJET TOTAL-PRESSURE LOSSES

The flameholder drag losses are determined by assuming that the total-pressure drop is equal to 4 times the velocity head and solving in terms of the Mach number at station 3 (relative to rotating coordinates):

$$p_2'' - p_3'' = 4q \tag{B1}$$

where

$$q = p_2'' - p_2 = p_2 \left[\left(1 + \frac{k - 1}{2} M_2^2\right)^{\frac{k}{k-1}} - 1\right] \tag{B2}$$

Substituting for q in equation (B1) gives

$$p_2'' - p_3'' = 4p_2 \left[\left(1 + \frac{k - 1}{2} M_2^2\right)^{\frac{k}{k-1}} - 1\right]$$

$$\frac{p_3''}{p_2''} = 1 - 4\left[1 - \frac{1}{\left(1 + \frac{k - 1}{2} M_2^2\right)^{\frac{k}{k-1}}}\right] \tag{B3}$$

Expanding the Mach number function for $k = 1.4$,

$$\frac{1}{\left(1 + \frac{k - 1}{2} M_2^2\right)^{\frac{k}{k-1}}} \cong 1 - 0.7M_2^2 \tag{B4}$$

Substituting in equation (B3) yields

$$\frac{p_3''}{p_2''} \cong 1 - 2.8M_2^2 \tag{B5}$$

From the continuity equation for $M_2 << 1$,

$$\frac{M_3}{M_2} \cong \frac{p_2''}{p_3''}$$

and

$$M_2 \cong M_3 \frac{p_3''}{p_2''}$$

3668

Equation (B5) now becomes

$$\frac{p_3''}{p_2''} \cong 1 - 2.8 \left(\frac{p_3''}{p_2''}\right)^2 M_3^2 \tag{B6}$$

Solving the quadratic for p_3''/p_2'', the expression for the total-pressure ratio across the flameholder is

$$\frac{p_3''}{p_2''} \cong \frac{\sqrt{1 + 11.2\, M_3^2} - 1}{5.6\, M_3^2} \tag{7}$$

For an adiabatic expansion, the relation between total- and static-pressure ratios is given by

$$\frac{p_4''}{p_{3a}''} = \frac{p_4}{p_{3a}} \left(\frac{T_{3a}}{T_4}\right)^{\frac{k}{k-1}} \tag{B7}$$

and, since $T_4'' = T_{3a}''$,

$$T_{3a} + \frac{W_{3a}^2}{2gJc_p} = T_4 + \frac{W_4^2}{2gJc_p}$$

and

$$\frac{T_4}{T_{3a}} = 1 - \frac{W_4^2 - W_{3a}^2}{2gJc_pT_{3a}} \tag{B8}$$

For an expansion through the reaction turbine with losses,

$$\frac{W_4^2 - W_{3a}^2}{2gJc_p} = \eta_n T_{3a}\left[1 - \left(\frac{p_4}{p_{3a}}\right)^{\frac{k-1}{k}}\right] \tag{B9}$$

3668

where

$$\eta_n = \frac{W_4^2 - W_{3a}^2}{W_{4,i}^2 - W_{3a}^2}$$

Combining equations (B7) and (B8) and substituting in equation (B9) give the total-pressure ratio across the turbine nozzles:

$$\frac{p''_{3a}}{p''_4} = \left[\left(\frac{p_{3a}}{p_4}\right)^{\frac{k-1}{k}}(1 - \eta_n) + \eta_n\right]^{\frac{k}{k-1}} \tag{8}$$

REFERENCES

1. Breitwieser, Roland, Gordon, Sanford, and Gammon, Benson: Summary Report on an Analytical Evaluation of Air and Fuel Specific-Impulse Characteristics of Several Nonhydrocarbon Jet-Engine Fuels. NACA RM E52L08, 1953.

2. Henneberry, Hugh M.: Effect of Fuel Density and Heating Value on Ram-Jet Airplane Range. NACA RM E51L21, 1952.

3. Olson, Walter T., and Gibbons, Louis C.: Status of Combustion Research on High-Energy Fuels for Ram Jets. NACA RM E51D23, 1951.

4. Hurd, D. T.: Some Combustion Studies on Diborane. Rep. No. 55223, Res. Lab., General Electric Co., Sept. 22, 1947. (Proj. Hermes (TU1-2000), Ord. Dept.)

5. Anon.: Technical Data on Allegheny Ludlum Alloy S-816. Allegheny Ludlum Steel Corp., Watervliet (N.Y.), Jan. 3, 1950.

6. Cohen, Leo: Theoretical Investigation of Velocity Diagrams of a Single-Stage Turbine for a Turbojet Engine at Maximum Thrust per Square-Foot Turbine Frontal Area. NACA TN 2732, 1952.

7. Plohr, Henry W., and Hauser, Cavour H.: A Two-Dimensional Cascade Study of the Aerodynamic Characteristics of a Turbine-Rotor Blade Suitable for Air Cooling. NACA RM E51G18, 1951.

8. Cavicchi, Richard H., and English, Robert E.: A Rapid Method for Use in Design of Turbines within Specified Aerodynamic Limits. NACA TN 2905, 1953.

9. Zettle, Eugene V., and Friedman, Robert: Performance of Experimental Channeled-Wall Annulus Turbojet Combustor at Conditions Simulating High-Altitude Supersonic Flight. I - U-Shaped Channel Walls for Secondary-Air Entry. NACA RM E54L21a, 1955.

3668

3668

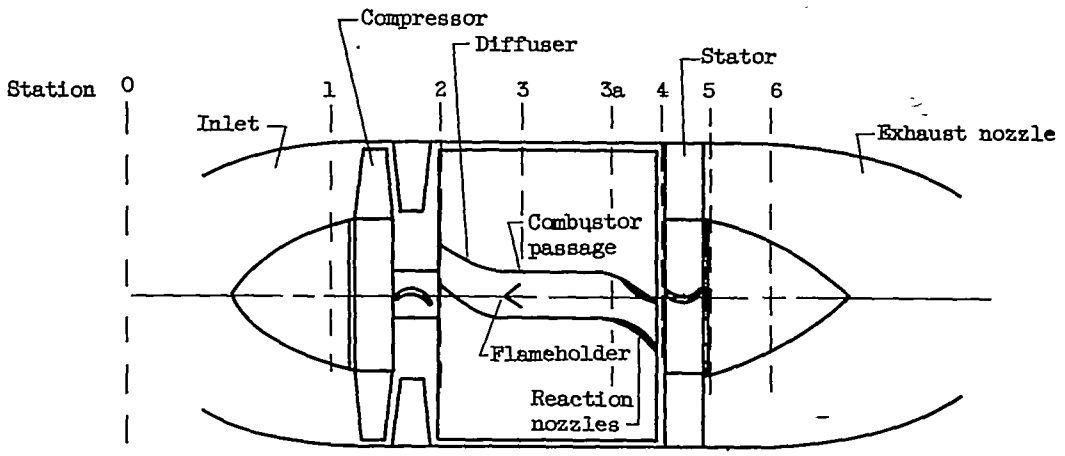

Figure 1. - Rotojet engine.

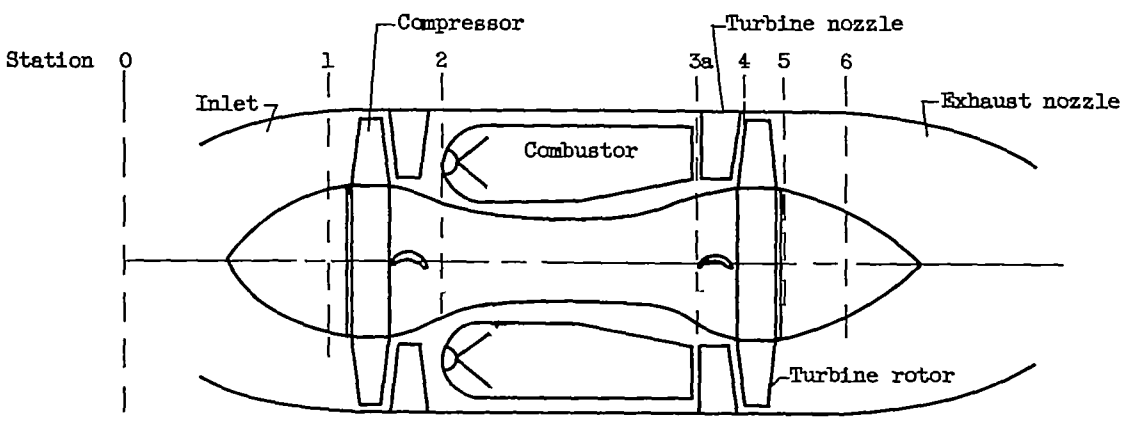

Figure 2. - Single-stage turbine engine.

3668

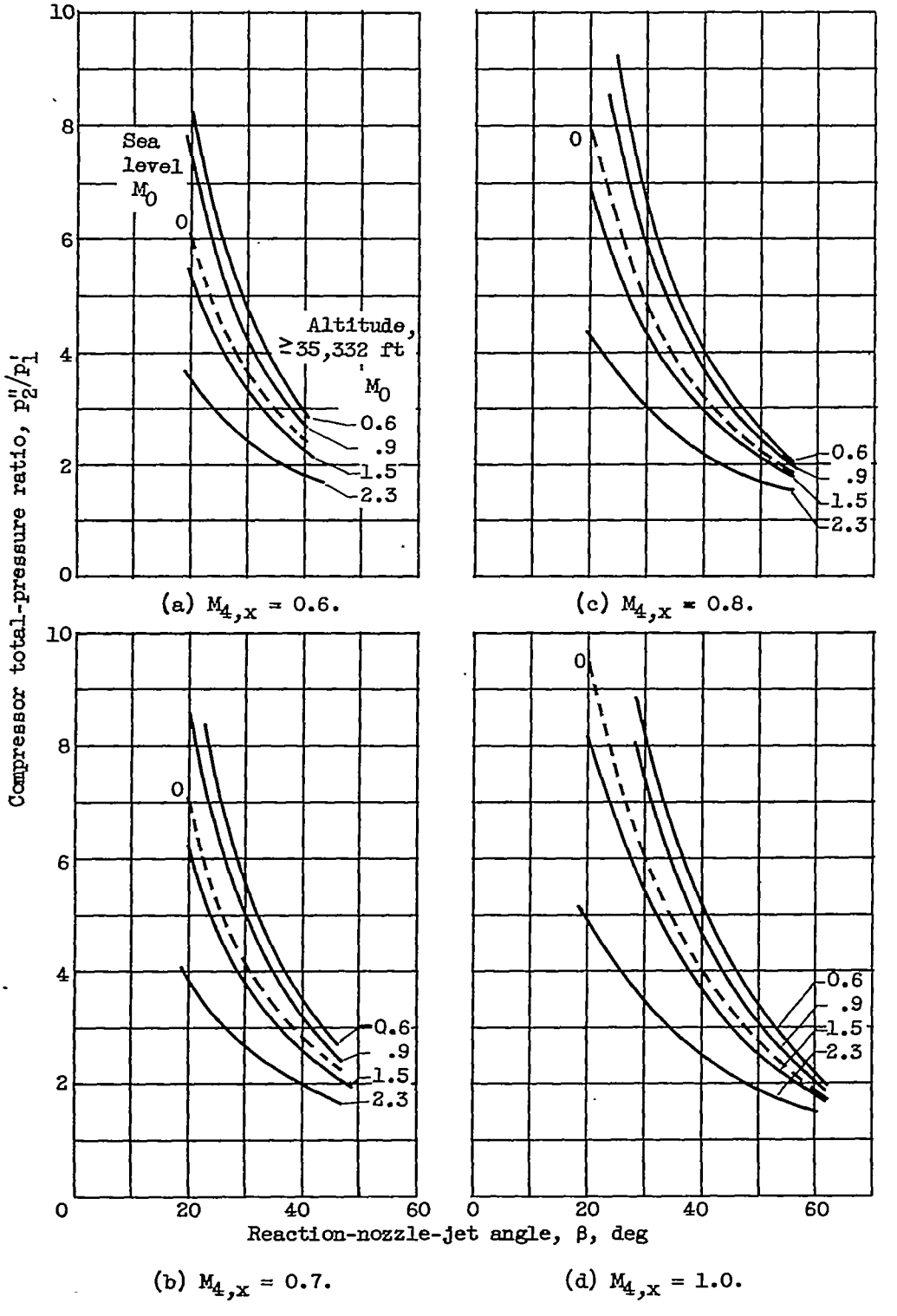

(a) $M_{4,x}$ = 0.6.

(b) $M_{4,x}$ = 0.7.

(c) $M_{4,x}$ = 0.8.

(d) $M_{4,x}$ = 1.0.

Figure 3. - Effect of reaction-nozzle-jet angle and turbine-exit axial Mach number on rotojet compression ratio. Turbine-inlet total temperature, 2500° R.

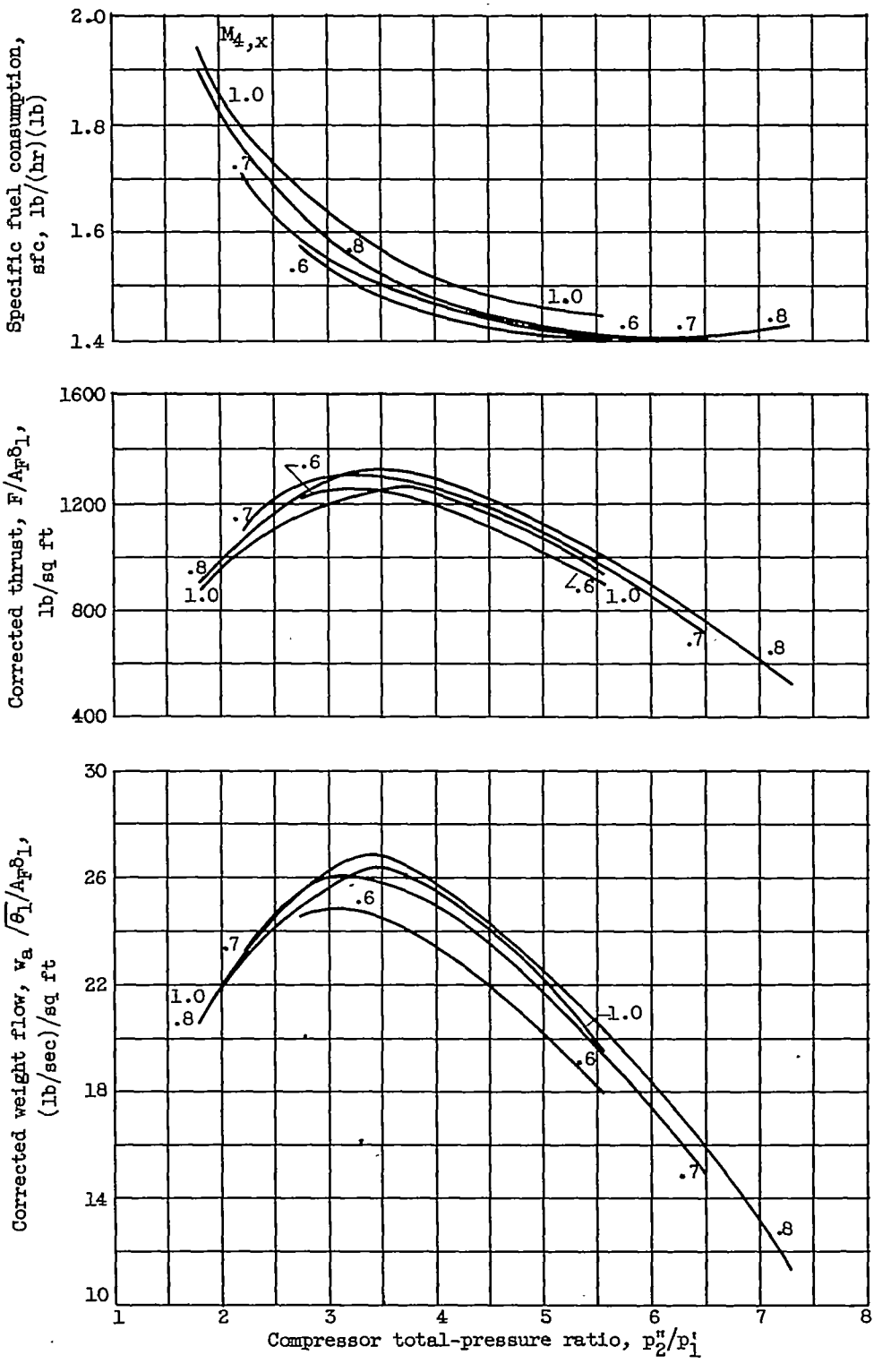

Figure 4. - Effect of turbine-exit axial Mach number on rotojet performance. Flight Mach number, 1.5; altitude, ≥35,332 feet. turbine-inlet total temperature, 2500° R.

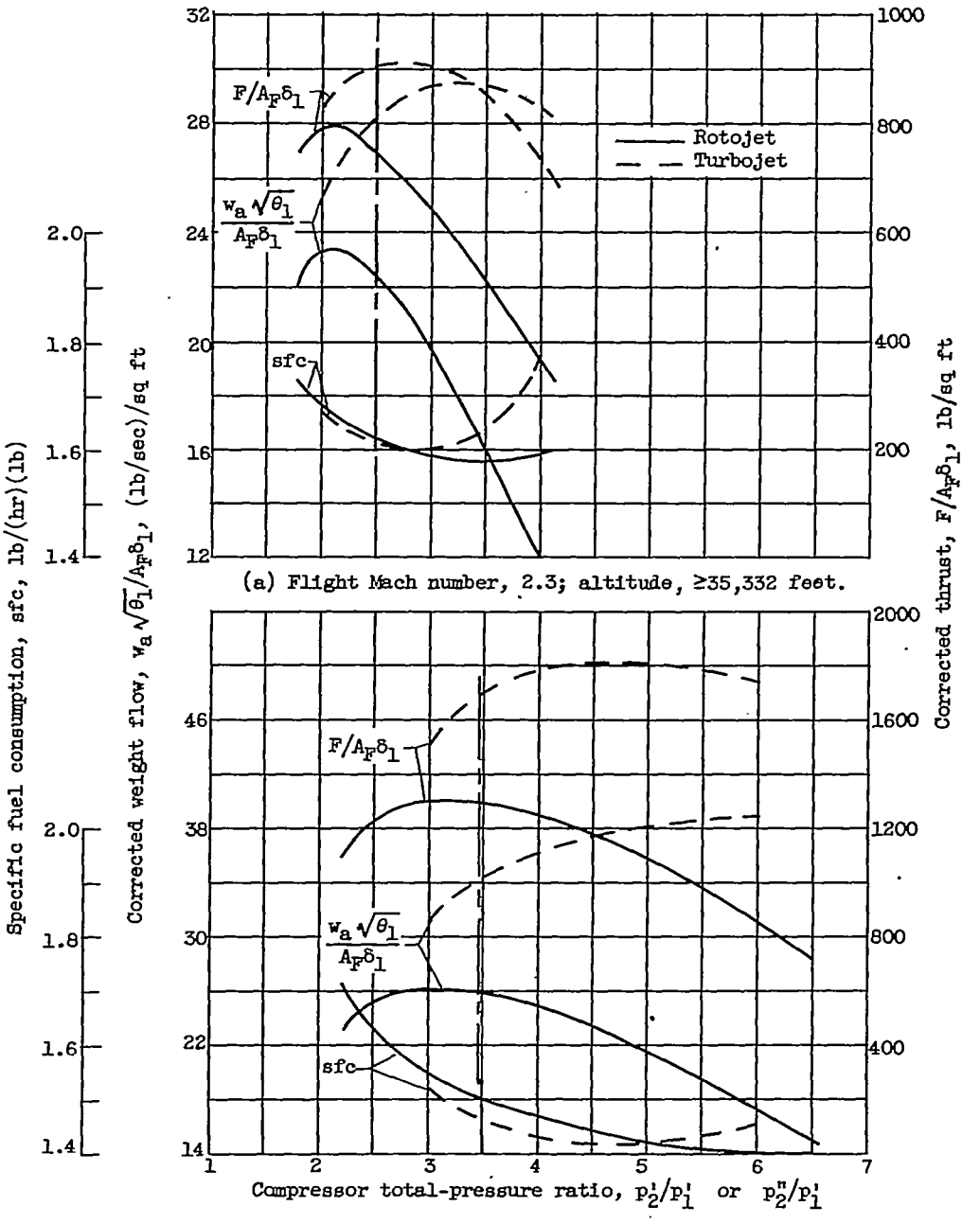

(a) Flight Mach number, 2.3; altitude, ≥35,332 feet.

(b) Flight Mach number, 1.5; altitude, ≥35,332 feet.

Figure 5. - Comparison of rotojet and turbojet performance at turbine-inlet total temperature of 2500° R.

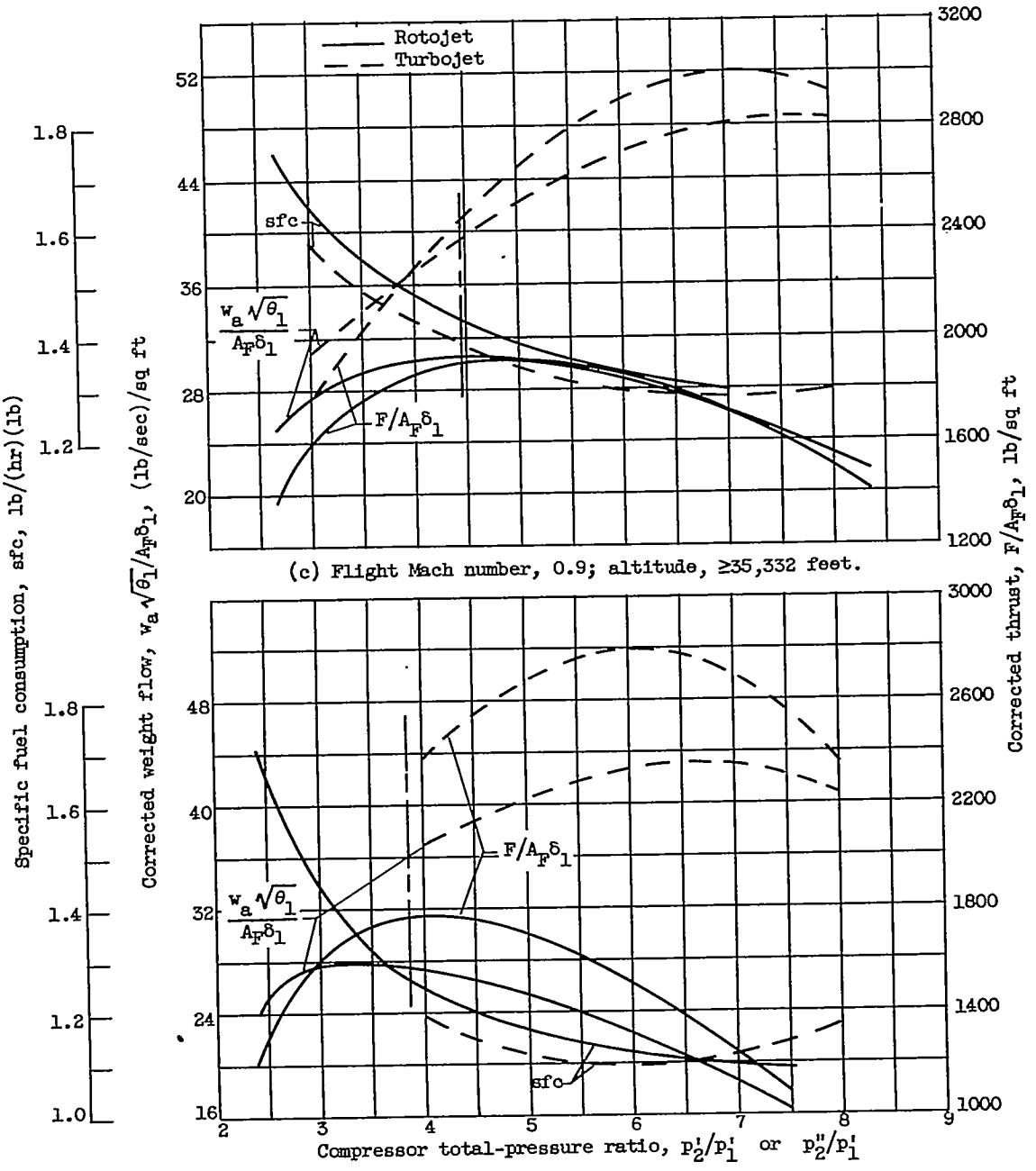

(c) Flight Mach number, 0.9; altitude, ≥35,332 feet.

(d) Flight Mach number, 0; sea level.

Figure 5. - Concluded. Comparison of rotojet and turbojet performance at turbine-inlet total temperature of 2500° R.

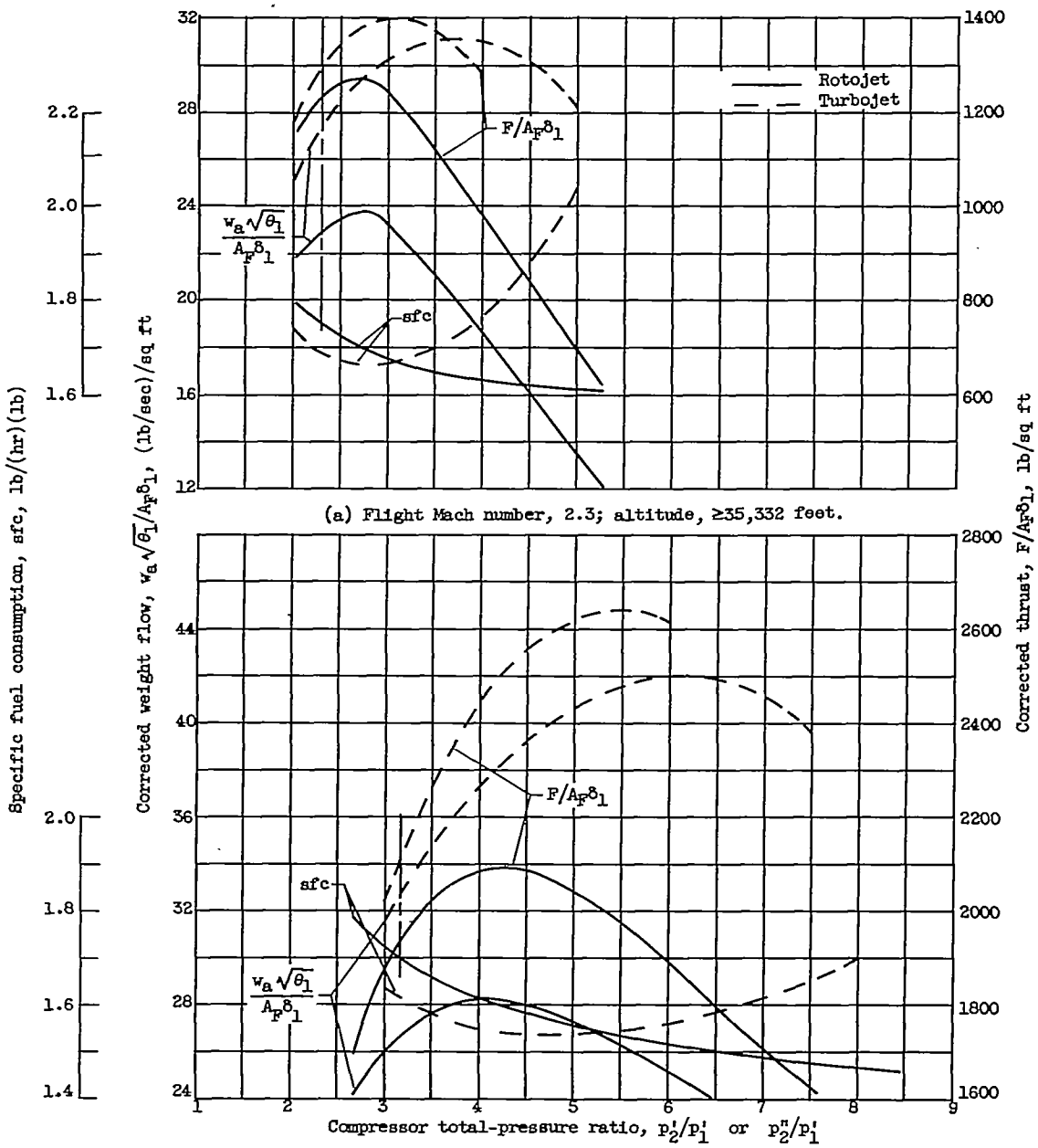

(a) Flight Mach number, 2.3; altitude, ≥35,332 feet.

(b) Flight Mach number, 1.5; altitude, ≥35,332 feet.

Figure 6. - Comparison of rotojet and turbojet performance at turbine-inlet total temperature of 3500° R.

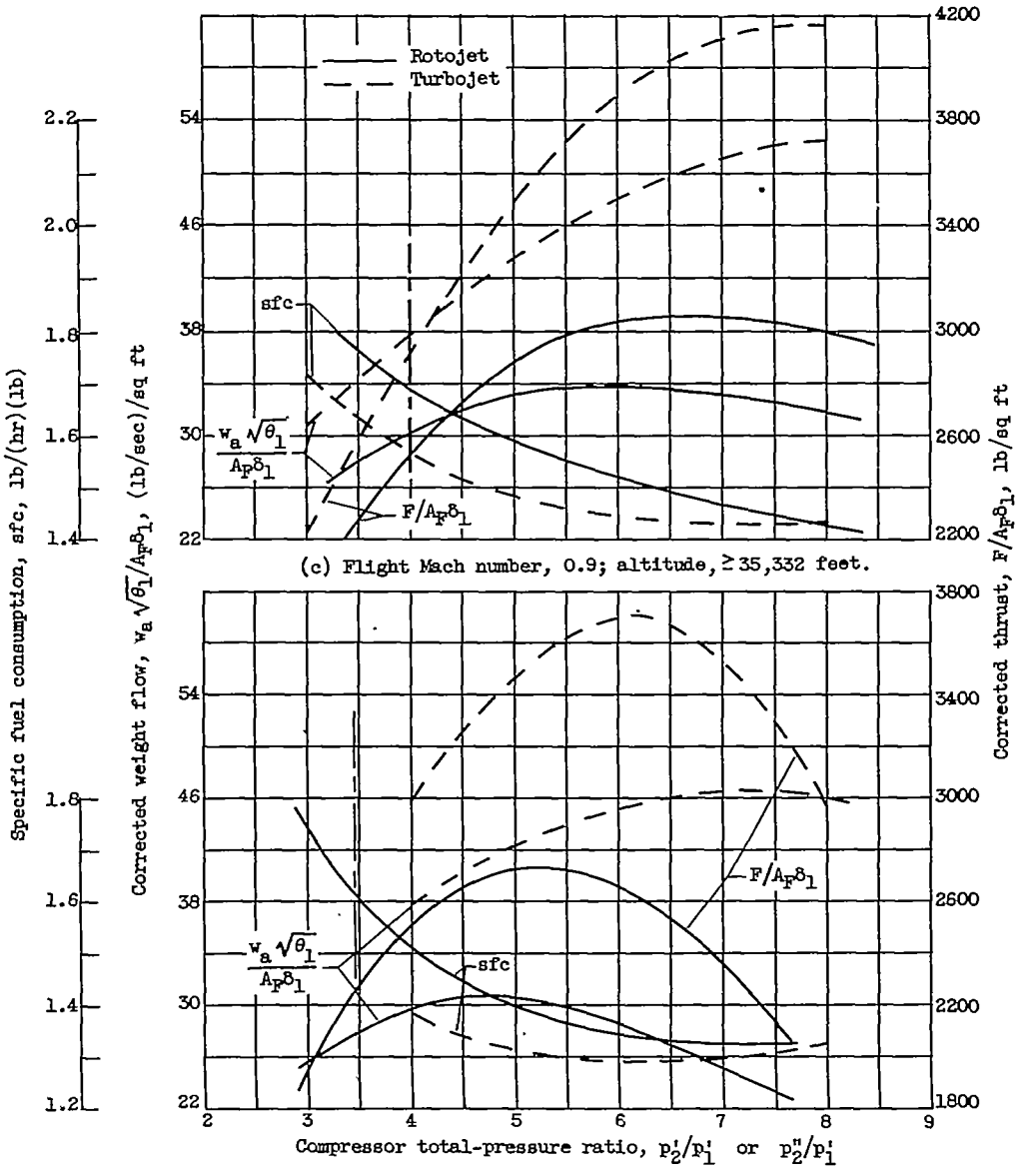

(c) Flight Mach number, 0.9; altitude, ≥35,332 feet.

(d) Flight Mach number, 0; sea level.

Figure 6. - Concluded. Comparison of rotojet and turbojet performance at turbine-inlet total temperature of 3500° R.

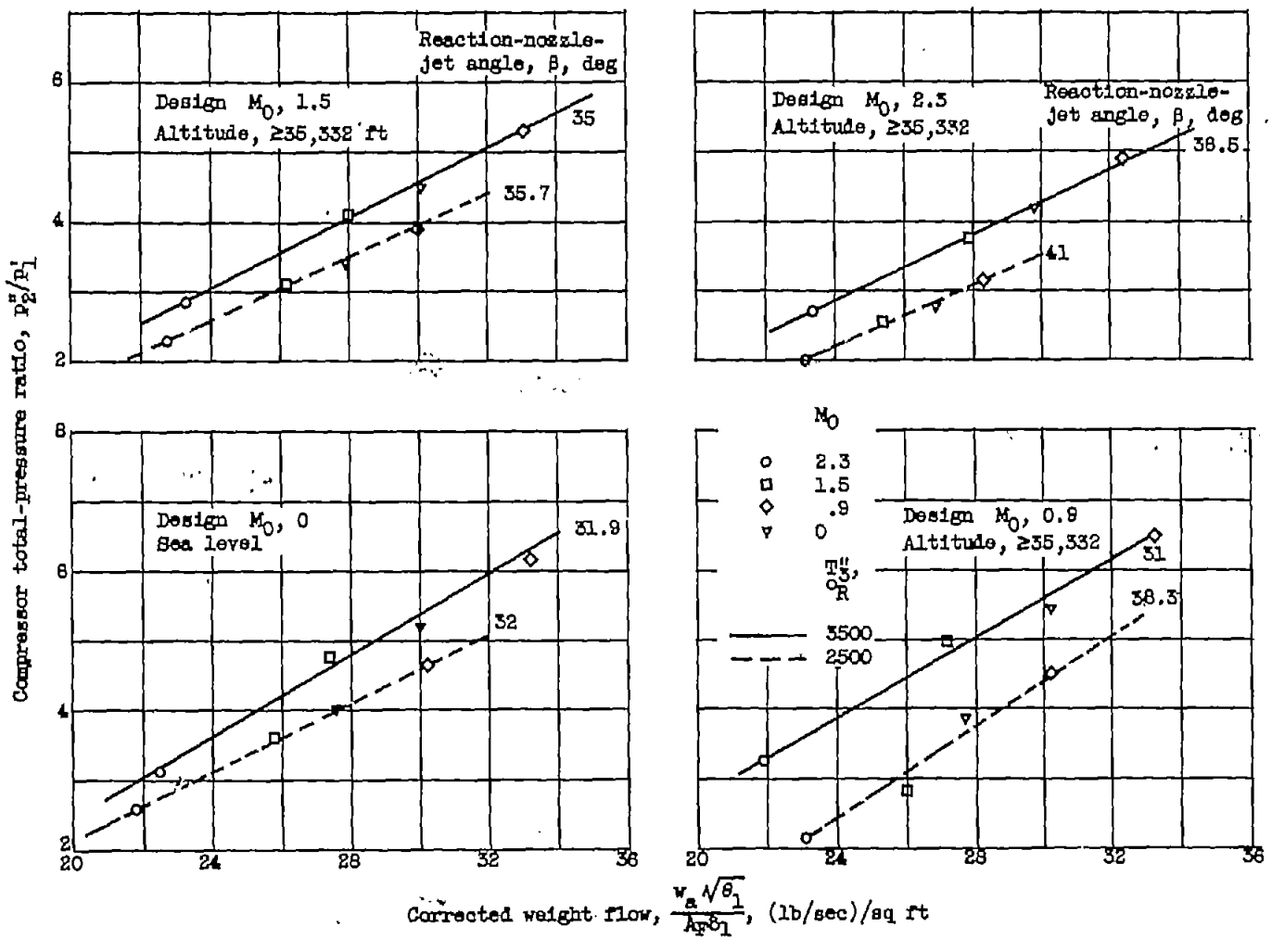

Figure 7. - Effect of fixed-geometry operation on weight-flow limitations of rotojet engine.